

Measurement of muscle protein synthesis by positron emission tomography with L-[methyl-¹¹C]methionine

(hind limb/arterio-venous difference/stable isotope/paraspinal muscle/dog)

HONGBING HSU*, YONG M. YU^{†‡}, JOHN W. BABICH*, JOHN F. BURKE^{†‡}, E. LIVNI*, RONALD G. TOMPKINS^{†‡},
VERNON R. YOUNG^{†‡}, NATHANIEL M. ALPERT*, AND ALAN J. FISCHMAN*^{‡§}

*Division of Nuclear Medicine of the Department of Radiology and [†]Trauma Service of the Department of Surgery, Massachusetts General Hospital and Harvard Medical School, Boston, MA; and [‡]Shriners Burns Institute, Boston, MA

Contributed by Vernon R. Young, November 8, 1995

ABSTRACT Positron emission tomography (PET) with L-[methyl-¹¹C]methionine was explored as an *in vivo*, noninvasive, quantitative method for measuring the protein synthesis rate (PSR) in paraspinal and hind limb muscles of anesthetized dogs. Approximately 25 mCi (1 Ci = 37 GBq) of L-[methyl-¹¹C]methionine was injected intravenously, and serial images and arterial blood samples were acquired over 90 min. Data analysis was performed by fitting tissue- and metabolite-corrected arterial blood time-activity curves to a three-compartment model and assuming insignificant transamination and transmethylation in this tissue. PSR was calculated from fitted parameter values and plasma methionine concentrations. PSRs measured by PET were compared with arterio-venous (A-V) difference measurements across the hind limb during primed constant infusion (5–6 h) of L-[1-¹³C, methyl-²H₃]methionine. Results of PET measurements demonstrated similar PSRs for paraspinal and hind limb muscles: 0.172 ± 0.062 vs. 0.208 ± 0.048 nmol⁻¹·min⁻¹·(g of muscle)⁻¹ ($P =$ not significant). PSR determined by the stable isotope technique was 0.27 ± 0.050 nmol⁻¹·min⁻¹·(g of leg tissue)⁻¹ ($P < 0.07$ from PET) and indicated that the contribution of transmethylation to total hind limb methionine utilization was $\approx 10\%$. High levels of L-[methyl-¹¹C]methionine utilization by bone marrow were observed. We conclude that muscle PSR can be measured *in vivo* by PET and that this approach offers promise for application in human metabolic studies.

Body protein wasting is a significant contributor to morbidity and death in a variety of catabolic disease states (1), with the major source of this loss being skeletal muscle (2, 3). Thus, a detailed and quantitative understanding of the regional distribution of protein and amino acid utilization and the ways by which imbalances between protein synthesis and breakdown occur in the major organs and their interactions should help to develop more effective nutritional/pharmacological strategies for attenuating these losses (4). Hitherto, relatively invasive techniques have been used to study local changes in protein and amino acid metabolism in animal models as well as in healthy humans (5–7), but their applicability in studies involving severely ill patients is problematic. To date, the principal technique that has yielded quantitative information about whole-body and regional aspects of amino acid metabolism in humans is based on measurements with stable isotope tracers (7–9). A method for the noninvasive, quantitative analysis of the regional distribution of amino acid metabolism, particularly in the musculature, in humans would be of considerable scientific value and of potential clinical importance.

A promising technique for noninvasive evaluation of tissue and organ metabolism is positron emission tomography (PET).

The publication costs of this article were defrayed in part by page charge payment. This article must therefore be hereby marked "advertisement" in accordance with 18 U.S.C. §1734 solely to indicate this fact.

The spatial resolution and quantitative nature of PET allows absolute quantification of metabolic parameters in volumes of tissue as small as a 1.0 cm³. PET techniques have been extensively validated for the measurement of regional blood flow, blood volume, oxygen utilization, and glucose metabolism in the brain and myocardium (10, 11). Although PET has not been applied previously in studies of mammalian amino acid metabolism in peripheral tissues, there are potentially attractive opportunities for the use of PET in the study of protein/amino acid metabolism-nutrition, particularly by making sequential time-dependent physiological and biochemical measurements in the same subject (12). More importantly, because of the relatively noninvasive nature of PET, measurements in human subjects can be made quite routine.

Studies with L-[methyl-¹¹C]methionine ([¹¹C]methionine) have indicated that it is a useful tracer for evaluation of amino acid kinetics *in vivo* and for detecting tumors (13–15). Further, it has been shown that isoenzymes of methionine adenosyltransferase, which catalyzes synthesis of *S*-adenosylmethionine, are active in liver, kidney, and bone marrow. However, compared with liver, the specific activity of this enzyme is about 30-fold lower in heart and skeletal muscle (16, 17). Therefore, most of the radioactivity that is retained in skeletal muscle following a dose of [¹¹C]methionine can be taken as an index of its incorporation into proteins. Also, for muscle, in contrast to some other ¹¹C-labeled tracers, such as [1-¹¹C]leucine, analysis of PET studies with [¹¹C]methionine is not complicated by a contribution of ¹¹CO₂ to total blood radioactivity (18). Thus, [¹¹C]methionine could be a valuable tracer for the quantitative analysis of muscle protein metabolism in human subjects under various pathophysiological states.

Hence, to establish a basis for the design and conduct of a series of studies in healthy adult control subjects and in different groups of hospitalized patients, we have studied the transport and metabolism of methionine in skeletal muscle of anesthetized dogs by PET using [¹¹C]methionine. Data analysis was performed by fitting tissue- and metabolite-corrected arterial blood time-activity curves to a three-compartment model. The model structure included: vascular space, tissue precursor, and protein compartments. The results of the PET measurements were compared with data from simultaneous studies using arterio-venous (A-V) difference measurements during primed constant infusion of L-[1-¹³C, methyl-²H₃]methionine [¹³C, ²H₃]methionine. This A-V difference isotope tracer approach has been applied by various investi-

Abbreviations: PET, positron emission tomography; A-V, arterio-venous; PSR, protein synthesis rate; [¹¹C]methionine, L-[methyl-¹¹C]methionine; [¹³C, ²H₃]methionine, L-[1-¹³C, methyl-²H₃]methionine. [§]To whom reprint requests should be addressed at: Division of Nuclear Medicine, Department of Radiology, Massachusetts General Hospital, 32 Fruit Street, Boston, MA 02114.

gators to quantify muscle protein metabolism within the limbs of human subjects (19–21).

MATERIALS AND METHODS

Preparation of [¹⁴C]methionine. [¹⁴C]methionine was prepared by the method of Langstrom *et al.* (22) with minor modifications. Radiochemical purity of the tracer was measured as described elsewhere (23) and was routinely >95%.

Animal Preparation. Seven conditioned male and female mongrel dogs, weighing 25–30 kg, were obtained from a commercial supplier (Buckshire Farms, Perkasie, PA) and housed in the Massachusetts General Hospital (MGH) animal farm. The dogs were cared for in accordance with the guidelines set forth by the Committee on Laboratory Resources, National Institutes of Health Council [DHEW (DHHS) publication no. 78-23] and the MGH Committee on Animal Research. Prior to the tracer studies, the animals were fasted overnight, and surgery was performed on the following morning by using aseptic techniques. The anesthesia used was an intravenous bolus of sodium pentobarbital (15 mg per kg of body weight) followed by a constant infusion (1 mg·kg⁻¹·hr⁻¹). The surgical procedures included implantation of polyethylene catheters (PE-90 or PE-260; Clay Adams) with silastic tips (Dow–Corning) into the jugular vein, the carotid artery, a deep vein of the left forelimb, the femoral artery, and the femoral vein. A blood-flow probe (size 2R, Transonic System, Ithaca, NY) was positioned around the left femoral artery.

Experimental Design. The kinetics of [¹⁴C]methionine and [¹³C-²H₃]methionine were studied in each dog as follows. At time 0 (baseline), samples of arterial and femoral venous blood and expired air were collected for analysis. This was followed by primed constant infusion of [¹³C, ²H₃]methionine for 5–6 hr. After the first 60 min of [¹³C, ²H₃]methionine infusion, a bolus of [¹⁴C]methionine was injected, blood sampling was started, and PET images of the paraspinal muscles were acquired for 90 min. The dog was then repositioned with the proximal hind limbs in the gantry of the PET camera. At ≈180 min of [¹³C, ²H₃]methionine infusion, a second bolus of [¹⁴C]methionine was injected, and blood sampling and PET imaging were repeated for 90 min. During the final hour of [¹³C, ²H₃]methionine infusion, plateau blood samples (left femoral artery and vein) were collected for measurements of methionine concentration and stable isotope enrichment in plasma-free methionine.

Blood Sampling for Radioactivity Measurements. Following [¹⁴C]methionine injection, arterial blood was sampled from the left carotid artery. Over the first 4 min, blood was withdrawn via a rotary pump (flow rate ≈ 8 ml·min⁻¹), and ¹⁴C radioactivity was recorded at 1-sec intervals with two pairs of on-line coincidence detectors. Thereafter, samples of arterial blood were withdrawn at 5, 10, 15, 30, 60, and 90 min, and radioactivity was measured in a well counter. “Metabolite-corrected” plasma time–activity curves were generated by multiplying the whole-blood time–activity curves by a metabolite correction function, which was obtained by fitting a biexponential function to the fraction of whole-blood radioactivity present as free [¹⁴C]methionine. This correction accounted for ¹⁴C radioactivity in blood cells, plasma proteins, and labeled metabolites (which we did not attempt to identify).

PET Imaging. The anesthetized and mechanically ventilated dogs were positioned and stabilized in the gantry of a PC-4096 plus PET camera [Scanditronix, Uppsala (24)]. The primary imaging characteristics of the PC-4096 camera are in-plane and axial resolutions of ≈6-mm full width at half maximum, 15 contiguous slices of 6.5-mm separation, and a sensitivity of ≈5,000 cps/μCi.

Approximately 25 mCi of [¹⁴C]methionine (specific activity ≈ 1,000 mCi/mmol) was injected as a sharp bolus through a forelimb venous catheter, and sequential images were acquired

over 90 min. The images were reconstructed by using a filtered-back projection algorithm. Data for attenuation correction were collected prior to the study with a ⁶⁸Ga rotating pin source. All projection data were corrected for nonuniformity of detector response, dead time, random coincidences, and scattered radiation. The PET camera was cross-calibrated to the well scintillation counter by comparing the PET camera response from a uniform distribution of a ¹⁸F solution in a 20-cm cylindrical phantom with the response of the well counter to an aliquot of the same solution.

Four to six irregular shaped regions of interest (ROIs), each containing ≈6 cm³ of tissue, were placed on selected slices. In positioning the ROIs, particular caution was taken to exclude bone and major vascular structures. The concentration of radioactivity in all of the ROIs was averaged to yield composite time activity curves (TACs).

Stable Isotope Measurements. Estimates of limb protein synthesis and breakdown were made on the basis of a 5- to 6-hr primed (6.4 μmol·kg⁻¹) constant infusion (0.09 μmol·kg⁻¹·min⁻¹) of [¹³C, ²H₃]methionine (MassTrace Inc. Woburn MA) and measurement of the A–V difference of methionine and its isotopic abundance by methods that are in routine use in our laboratory (5, 25). The loss of the [¹³C]carboxyl moiety of methionine as ¹³CO₂ in blood via trans-sulfuration (17) was not measured for technical reasons. Hence, we estimated homocysteine remethylation (26, 27) as an index of transmethylation activity on the assumption that there would be little oxidation of methionine in muscle, which is based on enzymatic (17) and tracer (28) data. For estimating limb protein synthesis from methionine, we assumed a methionine concentration of 121 μmol per g of mixed protein (29). Thus, the protein synthesis rate (PSR_{A–V}, μmol of methionine incorporated per unit of time) was estimated by means of the following equation:

$$PSR_{A-V} = \frac{[A]_{[^{13}C]Met} - [V]_{[^{13}C]Met}}{[A]_{[^{13}C]Met}} [A] \cdot F, \quad [1]$$

where $[A]_{[^{13}C]Met}$ and $[V]_{[^{13}C]Met}$ represent the total [¹³C]methionine tracer (per ml) in arterial and femoral venous blood, respectively; $[A]$ is the total free methionine concentration (μM) in arterial blood; and F is the blood flow (ml·min⁻¹) within the limb.

At the end of the tracer study, the animal received an overdose of sodium pentobarbital and the left hind limb was removed at the hip joint and weighed.

[¹⁴C]Methionine Kinetic Modeling. The configuration of the compartmental model used for data analysis is illustrated in Fig. 1. The rate constants $k_{1,2}$ and $k_{2,1}$ represent forward and reverse transport of methionine between plasma and tissue, and $k_{2,3}$ represents incorporation of the label into proteins, nucleic acids, creatine, and lipids. Because of the expected low level of transmethylation in muscle (16, 17), $k_{2,3}$ reflects protein synthesis in this tissue. Radioactivity in the vascular compartment was represented by a blood volume fraction parameter. Thus, if the concentration of labeled tissue precursor and labeled protein are denoted by F and P , respec-

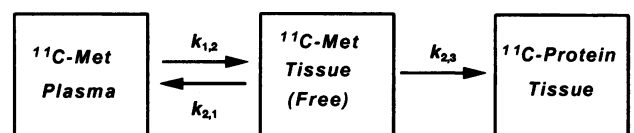


FIG. 1. Kinetic model for [¹⁴C]methionine (¹⁴C-Met) utilization by skeletal muscle. The model assumes that transamination and transmethylation are negligible and contains vascular space, tissue precursor, and protein compartments. The rate constants $k_{1,2}$ and $k_{2,1}$ represent forward and reverse transport of methionine between plasma and tissue, and $k_{2,3}$ represents incorporation into proteins.

tively, and the plasma concentration of labeled free methionine as a function of time is denoted by $C_p(t)$, then

$$\frac{dF}{dt} = k_{1,2}C_p(t) - (k_{2,1} + k_{2,3} + \lambda)F(t) \quad [2]$$

and

$$\frac{dP}{dt} = k_{2,3}F(t) - \lambda P(t), \quad [3]$$

where λ is the radioactive decay constant of ^{11}C .

The instantaneous tissue total radioactivity concentration as a function of time is given by

$$C_t(t) = (1 - b_v)[F(t) + P(t)] + b_v C_w(t), \quad [4]$$

where $C_w(t)$ is the measured whole-blood radioactivity as a function of time, and b_v is a parameter representing the fractional volume of the vascular space within the tissue.

The PET-measured tissue concentrations represent integrated average values over the duration of the scan as follows:

$$C_{\text{pet}}(t_i) = \frac{1}{\Delta t_i} \int_{t_{is}}^{t_{if}} C_t(t) dt, \quad [5]$$

where $C_{\text{pet}}(t_i)$ is the observed tissue concentration for a scan with an intermediate time t_i and starting and ending times t_{is} and t_{if} , respectively.

The model parameters were estimated by least-squares fitting of the predicted tissue concentrations of methionine [based on measured whole-blood ^{11}C radioactivity $[C_w(t)]$ and the concentration of free labeled methionine in plasma $[C_p(t)]$ to the tissue concentrations measured by PET.

By assuming steady-state conditions, the equilibrium concentration of free methionine in muscle can be calculated from the concentration of free methionine in plasma by using the following relation:

$$[\text{Tissue Met}] = \frac{k_{1,2}}{k_{2,1} + k_{2,3}} [\text{Met}], \quad [6]$$

where $[\text{Met}]$ denotes the plasma concentration of free methionine ($\text{nmol}\cdot\text{ml}^{-1}$).

Assuming that the density of muscle is $1.0 \text{ g}\cdot\text{ml}^{-1}$, protein synthesis rate (PSR, $\text{nmol}\cdot\text{min}^{-1}\cdot\text{g}^{-1}$) was calculated as follows:

$$\text{PSR} = \frac{k_{1,2}k_{2,3}}{k_{2,1} + k_{2,3}} [\text{Met}]. \quad [7]$$

The tissue precursor turn over half-time ($t_{1/2}$) can be estimated as follows:

$$t_{1/2}(\text{tissue precursor}) = \frac{0.693}{k_{2,1} + k_{2,3}}. \quad [8]$$

Statistical Evaluations. Data were summarized as means \pm SD and comparisons were made by using paired or unpaired t tests and linear regression analysis.

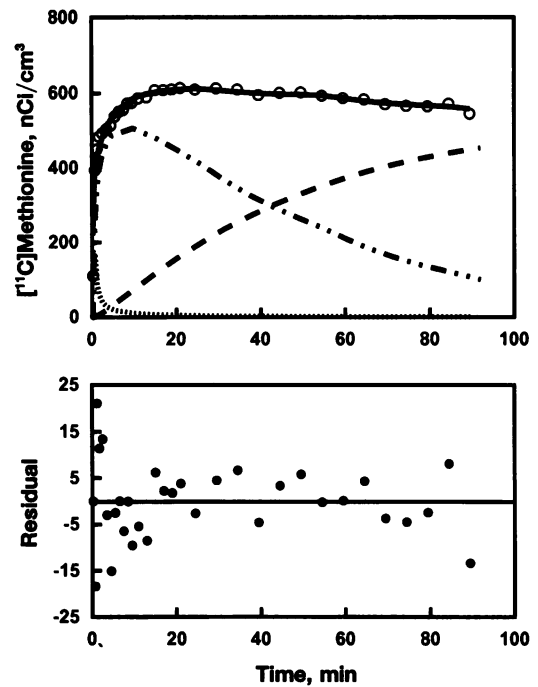


FIG. 2. (Upper) Typical least-squares fit of a PET time activity curve for the average concentration of $[^{11}\text{C}]$ methionine in hind limb muscle based on the kinetic model shown in Fig. 1 (solid curve and open circles). The time dependence of blood radioactivity (dots) and model estimates of concentrations of radioactivity in tissue free methionine (dot-dash) and labeled protein (dashes) compartments are also illustrated. (Lower) Time dependence of the residuals derived from the least-squares procedure (filled circles).

RESULTS

Fig. 2 shows a typical least-squares fit of a time-activity curve for the average concentration of $[^{11}\text{C}]$ methionine in hind limb muscle to the kinetic model presented in Fig. 1. The time dependence of the residuals derived from the least-squares procedure and model estimates of the concentrations of radioactivity in tissue free methionine and labeled protein compartments are also illustrated. All concentrations have been corrected for radioactive decay). These results show that the time dependence of the concentration of $[^{11}\text{C}]$ methionine in muscle is well described by the model. This is further supported by the random nature of the residuals.

Estimated model parameters and values for the PSR and $t_{1/2}$ of the tissue precursor pool for paraspinal and hind limb muscles are given in Table 1. Significant differences between hind limb and paraspinal muscles were not detected for $k_{1,2}$, $k_{2,1}$, $k_{2,3}$ PSR, or $t_{1/2}$. Further, one animal was given two doses of tracer separated by an interval of 120 min, and the PET measurements of hind limb PSRs agreed closely. Also, Fig. 3 demonstrates that PSRs calculated for hind limb and paraspinal muscle were highly correlated ($r^2 = 0.91$, $P < 0.001$).

Inspection of the PET images revealed that, compared with muscle, much higher concentrations of radioactivity accumulate in the bone marrow of most dogs (Fig. 4). To quantify the

Table 1. Kinetic parameters for $[^{11}\text{C}]$ methionine metabolism in paraspinal and hind limb muscles (mean \pm SD)

| Muscle | Animal samples, no. | $k_{1,2}$, $\text{ml}\cdot\text{min}^{-1}\cdot\text{g}^{-1}$ | $k_{2,1}$, min^{-1} | $k_{2,3}$, min^{-1} | $t_{1/2}^*$ | PSR, $\text{nmol}\cdot\text{min}^{-1}\cdot\text{g}^{-1}$ |
|------------|---------------------|---|-------------------------------|-------------------------------|------------------|--|
| Paraspinal | 5 | 0.0154 ± 0.0058 | 0.0266 ± 0.0094 | 0.0124 ± 0.0049 | 19.77 ± 7.35 | 0.172 ± 0.062 |
| Hind limb | 7 | 0.0170 ± 0.0055 | 0.0304 ± 0.0100 | 0.0155 ± 0.0058 | 16.51 ± 5.33 | 0.208 ± 0.048 |
| Total | 12 | 0.0164 ± 0.0054 | 0.0289 ± 0.0095 | 0.0143 ± 0.0055 | 17.76 ± 6.11 | 0.193 ± 0.054 |

* $t_{1/2} = 0.693 / (k_{2,1} + k_{2,3})$ (Eq. 8 in the text).

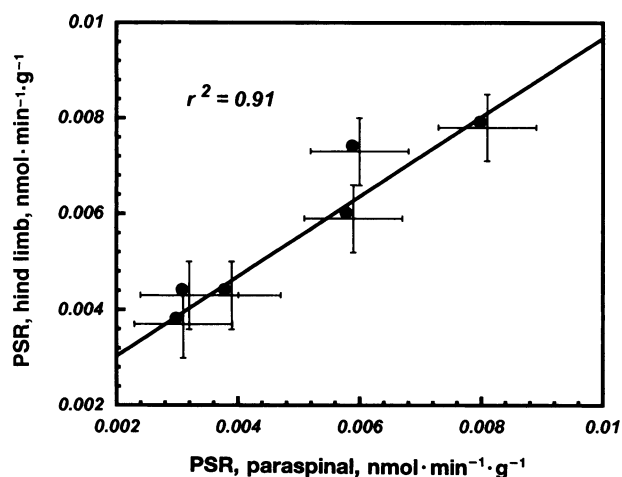


FIG. 3. Correlation between PSRs (mean \pm SD) determined by PET for hind limb and paraspinal muscle.

difference in methionine utilization between muscle and bone marrow, TACs for bone marrow were fitted to the same model. However, since transmethylation is expected to occur in bone marrow, compartment P would represent radioactivity incorporated both into proteins and methylated compounds. From this analysis, all three rate constants and PSR for bone marrow were significantly ($P < 0.005$, paired t test) greater than for muscle ($k_{1,2} = 0.11 \pm 0.06$, $k_{2,1} = 0.13 \pm 0.05$, $k_{2,3} = 0.049 \pm 0.017$, and $\text{PSR} = 1.14 \pm 0.65$). The tissue free methionine pools showed marked differences in turnover half-time, with $t_{1/2} = 4.9 \pm 3.6$ min for bone marrow and $t_{1/2} = 16.5 \pm 5.3$ min for hind limb muscle.

PSR in the limb was also determined by primed constant infusion of ^{13}C - $^2\text{H}_3$ -Met together with A-V difference measurements of methionine isotopomer concentrations across the hind limb. PSR values calculated from the net disappearance of the $1\text{-}^{13}\text{C}$ label were 0.27 ± 0.05 $\text{nmol} \cdot \text{min}^{-1} \cdot \text{g}^{-1}$. Fig. 5 illustrates the hind limb PSR and rate of remethylation. These data demonstrate that PSR, expressed in relation to the weight of limb tissue, is somewhat higher ($P < 0.07$) than the PET value. Since the stable isotope procedure measures methionine utilization across the entire limb, at least some of the difference may be explained by bone marrow metabolism

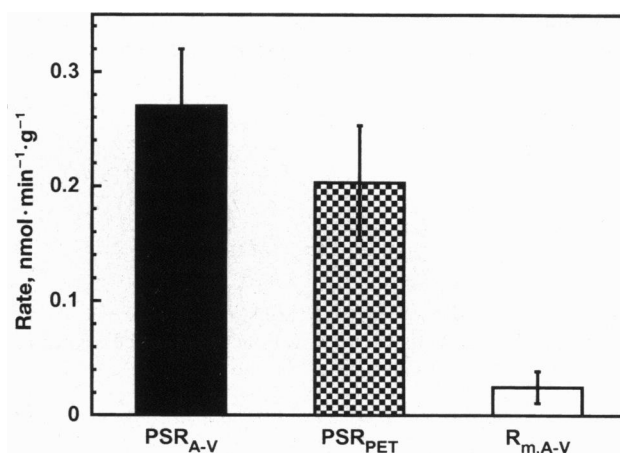


FIG. 5. A-V difference measurements of protein synthesis rate ($\text{PSR}_{\text{A-V}}$) and transmethylation (R_{m}) performed by primed constant infusion of $[^{13}\text{C}, ^2\text{H}_3]\text{methionine}$. The PET measurement of PSR is reproduced for comparison. Each bar is the mean \pm SD ($n = 7$).

and the higher fractional rate of protein synthesis in the skin (30).

As also shown in Fig. 5, remethylation of homocysteine accounted for $< 10\%$ of the metabolic uptake of methionine by the whole limb. This supports our assumption that the rate of transmethylation of $[^{13}\text{C}]\text{methionine}$ would be low in this tissue. Additionally, these findings may be useful to dissect out the metabolic activity in bone marrow, as follows: by assuming that total hind limb utilization of methionine takes place in muscle, skin, and bone marrow and that transmethylation occurs only in the marrow, the following calculation can be used to estimate the quantitative fate of methionine in bone:

$$[\text{PSR} + R_{\text{m}}]_{\text{A-V}} = (1 - \alpha)M_{\text{PET}} + \alpha \cdot \text{BM}_{\text{PET}} \quad [9]$$

$$R_{\text{m,A-V}} = \alpha \cdot \beta \cdot \text{BM}_{\text{PET}}, \quad [10]$$

where M_{PET} and BM_{PET} are PET measurements of tracer utilization by muscle (combined with skin) and bone marrow, respectively; $\text{PSR}_{\text{A-V}}$ and $R_{\text{m,A-V}}$ are A-V difference measurements of whole-limb protein synthesis and remethylation (an index of the transmethylation rate); α is the fractional volume of bone marrow in the limb; and β is the fractional contribution of bone marrow methionine utilization via transmethylation.

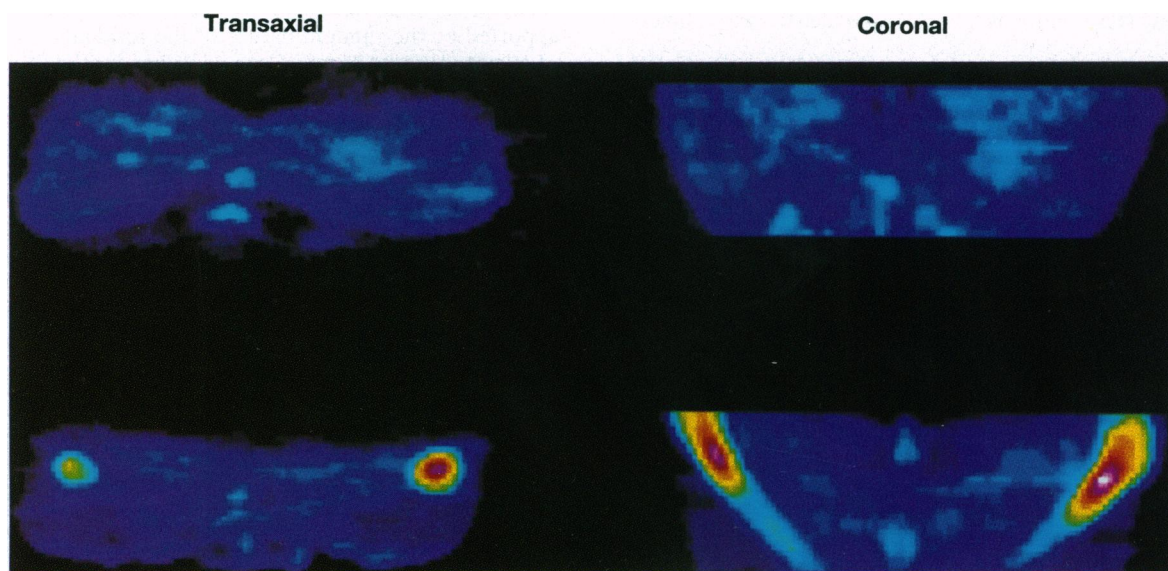


FIG. 4. Transverse (Left) and coronal (Right) PET images of the hind limbs of dogs with low (Upper) and high (Lower) accumulation of $[^{11}\text{C}]\text{methionine}$ in bone marrow.

Substitution of average values for the measured parameters yields values for α and β of 10% and 23%, respectively.

DISCUSSION

Quantitative aspects of amino acid utilization and protein synthesis in human subjects have been investigated extensively by intravenous or oral administration of stable isotope-labeled amino acids (8, 31). Although these studies have given information about whole-body metabolic rates, most have not provided estimates of amino acid metabolism in specific tissues and organs; the latter have been derived mostly from A–V difference studies (32). However, this approach has several limitations when applied to human studies: (i) measurements cannot be performed in tissues and organs that do not have a discrete venous drainage; (ii) for organs with a single venous drainage, the catheterization required for measuring A–V differences may be unsuitable for routine application; (iii) the measurements have limited anatomic resolution—i.e., A–V differences alone cannot be used to determine the individual contributions made by muscle, bone marrow, fat, and skin to substrate utilization; and (iv) relatively long infusion times (~5 hr) are required for many of these studies.

On the other hand, PET provides a routine noninvasive, *in vivo* method for the quantitative analysis of tissue-specific biochemical processes. Compared with the A–V difference techniques, PET has several advantages. (i) The measurements require only a metabolite-corrected arterial input function and imaging. (ii) The anatomic resolution of PET allows measurements to be performed on tissue volumes as small as 1.0 cm³. (iii) Because of the short half-lives of the tracers, repetitive studies can be performed in the same subject. The limitations of the PET methodology include (i) an exposure to ionizing radiation and (ii) inability to get a direct estimate of the specific metabolic pathways followed by the tracer. Thus, despite the wide use of [¹¹C]methionine as a tracer, quantitative estimation of cerebral protein synthesis with this tracer is problematic because of active transmethylation processes in this organ. In the case of the present study, however, [¹¹C]methionine was chosen because of the relatively low rates of methionine transmethylation and remethylation of homocysteine in muscle, permitting use of a simple three-compartmental model, similar to the earlier [¹⁸F]deoxyglucose model (33), to describe its metabolism.

The paraspinal and hind limb muscles were found to have similar PSRs, of ≈ 0.20 nmol of methionine incorporated per g of muscle per min. The mean estimate from [¹³C, ²H₃]methionine A–V tracer balance was 0.27 nmol per g of limb tissue per min. These comparable estimates are noteworthy because a major aim of this study was to establish the possible equivalence of these two approaches for estimation of *in vivo* rates of muscle protein synthesis. Based on the stable isotope and leg weight data, the rate of protein synthesis in the total hind limb was equivalent to 7.3 ± 1.7 (mean \pm SD) g·day⁻¹. This compares with the limited published values of about 3.2 g·day⁻¹ (34) and 8.6–11.5 g·day⁻¹ (35) for the hind limbs of dogs of comparable body weight. These differences are, in part, likely related to the blood flow rate across the limb during the study. Our PET measurements required that the leg be immobile. Hence, the dogs were heavily sedated and the hind limb restrained—procedures that could have affected regional blood flow and the status of protein and amino acid metabolism in the limb. Recent reviews (36, 37) emphasize the importance of blood flow on oxygen and substrate delivery in affecting metabolism in tissues and organs. In the present study, mean hind limb blood flow rate was 91 ml·min⁻¹, whereas, it was about 228–240 ml·min⁻¹ in studies by Biolo *et al.* (30, 35) and 33 ml·min⁻¹ in that of Barret *et al.* (34). At least, the limb protein synthesis rate measured in the present study is similar to these other reports when differences in blood flow rates are taken into consideration. Additionally, the primed

A–V difference method would tend to give a minimum estimate of PSR because the direct utilization of amino acids derived from protein breakdown for synthesis is not included.

In summary, muscle protein synthesis was measured by PET with [¹¹C]methionine. Comparison of PET and whole-limb stable isotope tracer A–V difference measurements indicated consistent estimates of the protein synthetic activity in this region. The stable isotope measurements also confirmed our assumption of a relatively low rate of methionine transmethylation in muscle; remethylation accounted for <10% of total methionine utilization in the leg. Overall, our results reveal that PET is a potentially useful technique for measuring local amino acid metabolism *in vivo* and that [¹¹C]methionine should be a suitable tracer for the noninvasive study of muscle protein synthesis in human subjects. Further, the high level of utilization of [¹¹C]methionine by bone marrow suggests that this tracer also may be useful for monitoring bone marrow metabolism in various pathological states as well as during radiation treatment and chemotherapy.

H.H. and Y.M.Y. contributed equally to conducting the experiments described here. The authors acknowledge the excellent technical support from Stephen Weise, Avis Loring, Michael Callaway, Susan Huang, Don Costa, and Eva Ambroz as well as the efforts of the Massachusetts General Hospital Cyclotron Laboratory. This work was supported in part by grants from the Shriners Hospitals for Crippled Children and the National Institutes of Health (P50-GM21700, T32-GM07035, and T32-CA09362).

- Hill, G. L. (1992) *Disorders in Nutrition and Metabolism in Clinical Surgery* (Churchill Livingstone, Edinburgh).
- Rennie, M. J. (1985) *Br. Med. Bull.* **41**, 257–304.
- Kinney, J. M. & Elwyn, D. H. (1983) *Annu. Rev. Nutr.* **3**, 433–466.
- Zeigler, T. R., Gatzen, C. & Wilmore, D. W. (1994) *Annu. Rev. Med.* **45**, 459–480.
- Yu, Y. M., Wagner, D. A., Tredget, E. E., Walaszewski, J. A., Burke, J. F. & Young, V. R. (1990) *Am. J. Physiol.* **259**, E36–E51.
- Deutz, N. E., Reijnen, P. L., Athanasas, G. & Soeters, P. B. (1992) *Clin. Sci.* **83**, 607–614.
- Matthews, D. E. & Bier, D. M. (1983) *Annu. Rev. Nutr.* **3**, 309–339.
- Waterlow, J. C. (1995) *Annu. Rev. Nutr.* **15**, 57–92.
- Young, V. R. (1987) *Am. J. Clin. Nutr.* **46**, 709–725.
- Mazziotta, J. C. & Phelps, M. E. (1986) in *Positron Emission Tomography and Autoradiography: Principles and Applications for the Brain and Heart*, eds. Phelps, M. E., Mazziotta, J. C. & Schelbert, H. R. (Raven, New York), pp. 493–579.
- Schelbert, H. R. & Schwaiger, M. (1986) in *Positron Emission Tomography and Autoradiography: Principles and Applications for the Brain and Heart*, eds. Phelps, M. E., Mazziotta, J. C. & Schelbert, H. R. (Raven, New York), pp. 581–661.
- Huang, S. C. & Phelps, M. E. (1986) in *Positron Emission Tomography and Autoradiography: Principles and Applications for the Brain and Heart*, eds. Phelps, M. E., Mazziotta, J. C. & Schelbert, H. R. (Raven, New York), pp. 287–346.
- Phelps, M. E., Barrio, J. R., Huang, S. C., Keen, R. E., Chugani, H. & Mazziotta, J. C. (1984) *Ann. Neurol.* **15**, Suppl., S192–S202.
- Ishiwata, K., Vaalburg, W., Elsinga, P. H., Paans, A. M. & Woldring, M. G. (1988) *J. Nucl. Med.* **29**, 1419–1427.
- Planas, A. M., Prenant, C., Mazoyer, B. M., Comar, D. & Di-Giamberardino, L. (1992) *J. Cereb. Blood Flow Metab.* **12**, 603–612.
- Mudd, S. H., Finkelstein, J. D., Irreverre, F. & Laster, L. (1965) *J. Biol. Chem.* **240**, 4382–4392.
- Finkelstein, J. D. (1990) *J. Nutr. Biochem.* **1**, 228–237.
- Hawkins, R. A., Huang, S. C., Barrio, J. R., Keen, R. E., Fong, D., Mazziotta, J. C. & Phelps, M. E. (1989) *J. Cereb. Blood Flow Metab.* **9**, 446–460.
- Cheng, K. N., Dworzak, F., Ford, G. C., Rennie, M. J. & Halliday, D. (1985) *Eur. J. Clin. Invest.* **15**, 349–354.
- Tessari, P., Inchiostro, S., Zanetti, M. & Barazzoni, R. (1995) *Am. J. Physiol.* **269**, E127–E136.
- Biolo, G., Fleming, R. Y. D. & Wolfe, R. R. (1995) *J. Clin. Invest.* **95**, 811–819.

22. Langstrom, B., Antoni, G., Gullberg, P., Halldin, C., Malmberg, P., Nagren, K., Rimland, A. & Svard, H. (1987) *J. Nucl. Med.* **28**, 1037–1040.
23. Nagren, K. (1993) in *PET Studies on Amino Acid Metabolism and Protein Synthesis*, eds. Mazoyer, B. M., Hess, W. D. & Comar, D. (Kluwer, Dordrecht, The Netherlands), pp. 87–87.
24. Rota Kops, E., Herzog, H., Schmid, A., Holte, S. & Feinendegen, L. E. (1990) *Comput. Assist. Tomogr.* **14**, 437–445.
25. Yu, Y. M., Young, V. R., Tompkins, R. G. & Burke, J. F. (1995) *J. Parenter. Enteral Nutr.* **19**, 209–215.
26. Storch, K. J., Wagner, D. A., Burke, J. F. & Young, V. R. (1988) *Am. J. Physiol.* **255**, E322–E331.
27. Storch, K. J., Wagner, D. A., Burke, J. F. & Young, V. R. (1990) *Am. J. Physiol.* **258**, E790–E798.
28. Goldberg, A. L. & Odessey, R. (1972) *Am. J. Physiol.* **223**, 1384–1391.
29. Stegink, L. D., Bell, E. F., Daabees, T. T., Anderson, D. W., Zike, W. L. & Filer, L. T., Jr. (1983) in *Amino Acids: Metabolism and Medical Applications*, eds. Blackburn, G. L., Grant, J. P. & Young, V. R. (Wright-PSG, Boston), pp. 123–146.
30. Biolo, G., Gastaldelli, A., Zhang, X.-J. & Wolfe, R. R. (1994) *Am. J. Physiol.* **267**, E467–E474.
31. Young, V. R., Yu, Y.-M. & Krempf, M. (1991) in *New Techniques in Nutritional Research*, eds. Whitehead, R. G. & Prentice, A. (Academic, San Diego), pp. 17–72.
32. Elia, M. (1991) *Nutr. Res. Rev.* **4**, 3–31.
33. Sokoloff, L., Reivich, M., Kennedy, C., Des Rosiers, M. H., Patlak, C. S., Pettigrew, K. D., Sakurada, O. & Shinohara, M. (1977) *J. Neurochem.* **28**, 897–916.
34. Barrett, E. T., Revkin, J. H., Young, L. H., Zaret, B. L., Jacob, R. & Gelfand, R. A. (1987) *Biochem. J.* **245**, 223–228.
35. Biolo, G., Chinkes, D., Zhang, X.-J. & Wolfe, R. R. (1992) *J. Parenter. Enteral Nutr.* **16**, 305–315.
36. Clark, M. G., Colquhoun, E. Q., Rattigan, S., Dora, K. A., Eldershaw, T. P. D., Hall, J. L. & Ye, J. (1995) *Am. J. Physiol.* **268**, E797–E812.
37. Elia, M. (1995) *Proc. Nutr. Soc.* **54**, 213–232.